

# Schelling's Segregation Model: Parameters, Scaling, and Aggregation

Abhinav Singh,<sup>1</sup> Dmitri Vainchtein,<sup>1\*</sup> Howard Weiss<sup>2</sup>

<sup>1</sup>School of Physics and Center for Nonlinear Science, Georgia Tech, USA

<sup>2</sup>School of Mathematics and Center for Nonlinear Science, Georgia Tech, USA

\*To whom correspondence should be addressed; E-mail: dmitri@gatech.edu.\*

**Thomas Schelling proposed an influential simple spatial model to illustrate how, even with relatively mild assumptions on each individual's nearest neighbor preferences, an integrated city would likely unravel to a segregated city, even if all individuals prefer integration. Aggregation relates to individuals coming together to form groups and global aggregation corresponds to segregation. Many authors assumed that the segregation which Schelling observed in simulations on very small cities persists for larger, realistic size cities. We devise new measures to quantify the segregation and unlock its dependence on city size, disparate neighbor comfortability threshold, and population density. We identify distinct scales of global aggregation, and show that the striking global aggregation Schelling observed is strictly a small city phenomenon. We also discover several scaling laws for the aggregation measures.**

---

\*This work was partially supported by NSF (grants DMS-0355180 and 0400370) and by the Donors of the ACS Petroleum Research Fund.

# 1 Introduction

In the 1970s, the eminent economic modeler Thomas Schelling proposed a simple space-time population model to illustrate how, even with relatively mild assumptions concerning every individual’s nearest neighbor preferences, an integrated city would likely unravel to a segregated city, even if all individuals prefer integration (6; 7; 8; 9). His agent based lattice model has become quite influential amongst social scientists, demographers, and economists, and a number of authors are testing the Schelling model using actual population data (13; 2; 1; 14). The only quantitative analysis of such models we could locate in the literature are (3) and (11).

Aggregation relates to individuals coming together to form groups or clusters according to race, and global aggregation corresponds to segregation. Many authors assume that the striking global aggregation observed in simulations on very small ideal “cities” persists for large, realistic size cities. A recent paper (10) exhibits final states for a small number of model simulations of a large city, and some final states that do not exhibit significant global aggregation. However, quantification of this important phenomenon is lacking in the literature, presumably, in part, due to the large computational costs required to run simulations using existing algorithms.

In this paper, we devise new measures to quantify the aggregation and unlock its dependence on city size, disparate neighbor comfortability threshold, and population density. We developed a highly efficient and fast algorithm that allows us to compute meaningful statistics of these measures (see Figures 3,8,10). We identify distinct scales of global aggregation, and we show that the striking global aggregation Schelling observed is strictly a small city phenomenon. We also discover several remarkable scaling laws for the aggregation measures.

## 1.1 Description of the Model

We expand Schelling’s original model<sup>1</sup> to a three parameter family of models. The phase space for these models is the  $N \times N$  square lattice with periodic boundary conditions. We consider two distinct populations, that, in Schelling’s words (9), refer to “membership in one of two homogeneous groups: men or women, blacks and whites, French-speaking and English speaking, officers and enlisted men, students and faculty, surfers and swimmers, the well dressed and the poorly dressed, and any other dichotomy that is exhaustive and recognizable.” We denote by B (black squares) and R (red squares) these two populations. See Figure 1. Together these agents fill up some of the  $N^2$  sites, with  $V$  remaining vacant sites (white squares). Each agent has eight nearest neighbors (Moore neighborhood). Fix a *disparate neighbor comfortability threshold*  $T \in \{0, 1, \dots, 8\}$ , and declare that a B or R is *happy* if  $T$  or more of its nearest eight neighbors are B’s or R’s, respectively. Else it is unhappy.

Demographically, the parameter  $N$  controls the size of the city,  $v = V/N^2$  controls the population density or the *occupancy ratio* (4), and  $T$  is an “agent comfortability index” that quantifies an agent’s tolerance to living amongst disparate nearest neighbors.

---

<sup>1</sup>Different authors frequently consider slightly different versions of Schelling’s original model, i.e., different ways of moving boundary agents. All versions seem to exhibit the same qualitative behaviors, and thus we refer to *the* Schelling model.

We begin the evolution by choosing an initial configuration (described in Sect. 3) and randomly selecting an unhappy B and a vacant site surrounded by at least  $T$  nearest B neighbors. Provided this is possible, interchange the unhappy B with the vacant site, so that this B becomes happy. Then randomly select an unhappy R and a vacant site having at least  $T$  nearest neighbors of type R. Provided this is possible, interchange the unhappy R with the vacant site, so that R becomes happy. Repeat this iterative procedure, alternating between selecting an unhappy B and an unhappy R, until a *final state* is reached, where no interchange is possible that increases happiness. For some final states, some (and in some cases, many) agents may be unhappy, but there are no allowable switches.

## 2 Schelling's results

Schelling considered the case  $N = 8, T = 3$ , and  $v = 33\%$ . The details of Schelling's simulations (including the algorithm for choosing initial conditions) are presented in Sec. 6.1 in the supporting materials. The final state of a typical run of Schelling's original model system is presented in Figs. 1. Schelling performed many simulations by hand using an actual checkerboard, and observed that the final states presented a significant degree of global aggregation. He equated the global aggregation with segregation of a city.

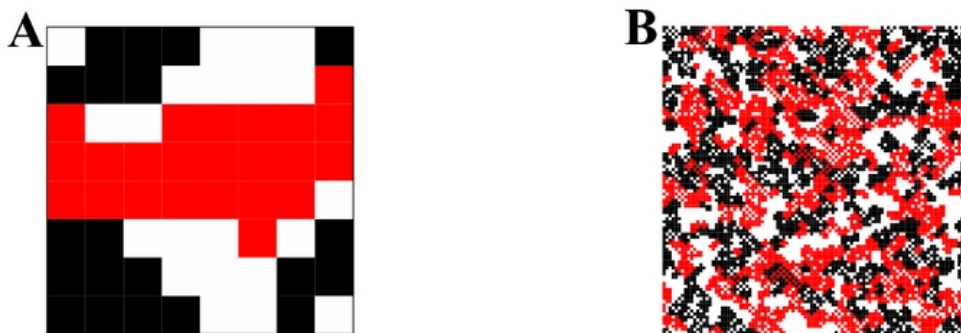


Figure 1: **A**: A simulation of Schelling's original model with  $N = 8$ ; **B**: Our simulation with  $N = 100$ .

In this paper, we investigate whether the global aggregation that Schelling observed for very small lattices persists for larger lattices. In Fig. 1**B**, we present a characteristic final state for our simulations with  $N = 100$ . Comparing Figs. 1**A** and 1**B**, one can see a striking qualitative difference between the two final states. While there is some local aggregation in the final state with  $N = 100$ , there is no global aggregation. By viewing the plots of this and other final states, one immediately sees that the global aggregation that Schelling observed is a small lattice phenomenon. In Sections 3 through 5 we quantify the global aggregation using several new measures, and we carefully analyze the structure of the final states for different values of  $T$  and  $v$ . In particular, we quantify the claim that global aggregation is a small lattice phenomenon.

### 3 Simulations

We study the dynamics for large lattices and present our results for  $N = 100$ . Figures 2-10 (except Fig. 4) are all based on  $N = 100$ . In the supporting materials, we discuss the cases  $N = 50$  and  $N = 200$ , and claim that  $N$  greater than 100 does not lead to qualitatively or quantitatively different states and phenomena. We restrict our discussion to cities having an equal number of B's and R's. A separate manuscript (12) will study the dynamics with different proportions of B's and R's.

We consider  $T = 3, 4, 5$  and  $v$  between 2% and 33%. The system does not evolve very much for other values of  $T$ : for  $T = 1, 2$  almost all of the agents are satisfied in most of the initial configurations, while for  $T \geq 6$  there are almost no legal switches. Values of  $v$  larger than 33% correspond to unrealistic environments. For each pair of parameters  $T$  and  $v$ , we perform 100 simulations (statistics are presented below and in the supporting materials). This number of simulations was chosen to ensure a 95% confidence interval for parameter estimation.

We choose the initial configuration by starting with a checkerboard with periodic boundary conditions. Demographically, a checkerboard configuration is a maximally integrated configuration. We then randomly remove  $V/2$  of both B's and R's (thus keeping equal numbers of both agents). We permute agents in two  $3 \times 3$  blocks. Alternatively, we could choose a random initial configuration. In general, except for small  $v$ , the final states are quantitatively similar as for our Schelling initial conditions.

In Fig. 2, we present characteristic final states for different values of  $T$  and  $v$ . Visually, the aggregation in the final states along each column (with fixed  $v$ ) is substantially different than in the final states along each row (with fixed  $T$ ). More characteristic final states are presented in Figs. 5-7 in the supporting materials. We begin the next section by defining several measures of aggregation that enable us to quantify this observation.

## 4 Analysis

### 4.1 Measures of Aggregation

One can see from Fig. 2 that aggregation is a multifaceted phenomenon, and thus requires several measures to describe. Schelling used two measures to quantify the aggregation: (1) the average over all agents of the quotient of the number of like to unlike neighbors, and (2) the number of agents whose eight nearest neighbors all have the same label, and thus are completely surrounded by like agents. We call the latter quantity *seclusiveness* and denote by  $N_0$ .

We introduce three additional measures. Aggregation manifests itself in two ways: (i) reduced number of contacts between agents of different kinds and (ii) the dominance of agents of either kind in a certain area. The first of the following measures of aggregation quantify (i) and the second and third measures quantify (ii).

(3) *The adjusted perimeter per agent  $p$  of the interface between the different agents suitably adjusted for the vacant spaces.* The adjusted perimeter is defined as twice the total number of R-B connections plus the total number of connections between R and B agents with vacant spaces,

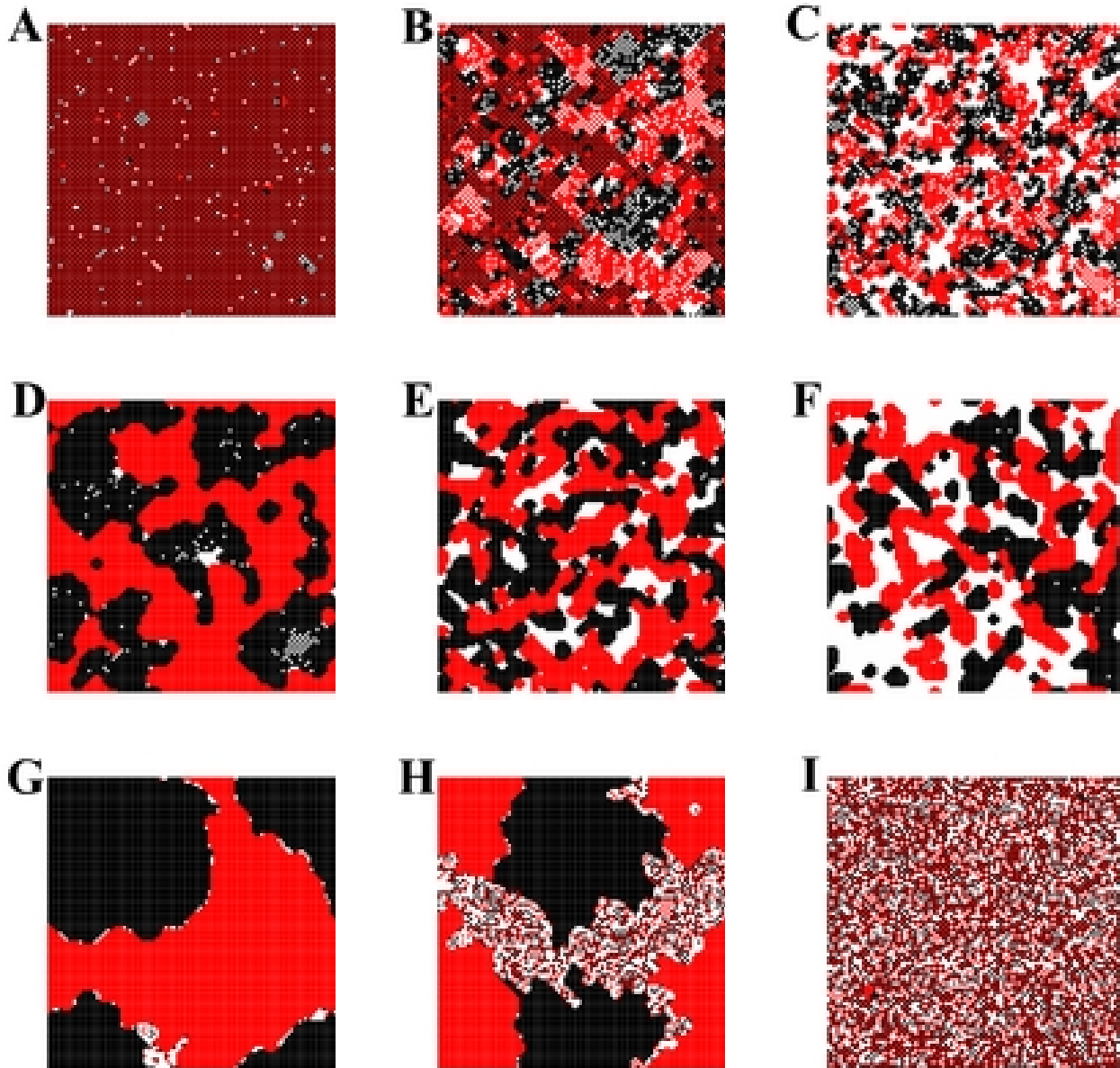


Figure 2: Characteristic final states for different values of  $T$  and  $v$ : **A:**  $T = 3, v = 2\%$ , **B:**  $T = 3, v = 15\%$ , **C:**  $T = 3, v = 33\%$ , **D:**  $T = 4, v = 2\%$ , **E:**  $T = 4, v = 15\%$ , **F:**  $T = 4, v = 33\%$ , **G:**  $T = 5, v = 2\%$ , **H:**  $T = 5, v = 15\%$ , **I:**  $T = 5, v = 33\%$ .

all divided by the total number of agents  $N^2$  (see the supporting materials). Demographically,  $p$  is the average number of contacts an agent has with the opposite kind or with vacant sites.

(4) *The scale, or maximum diameter of the connected components (which we henceforth call clusters)  $L$ .* The measure  $L$  is defined as the side length of the smallest square needed to cover every cluster. For states consisting of compact clusters, larger values of  $L$  correspond to larger *scales of aggregation*. Checkerboard configurations and configurations consisting of compact clusters are two extremes; for the former  $L = N$ .

(5) *The total number of clusters in a configuration  $N_C$ .* This intuitively appealing measure of aggregation is useful to describe final states having mostly large compact clusters. To see its limitation, observe that “the maximally integrated” checkerboard configuration with  $v = 0$  has just two clusters.

The definition of  $p$  was motivated by analogies of these models with the physics of foams. A key observation is that  $p$  is a Lyapunov function, i.e., a function defined on every configuration, and which is strictly decreasing along the evolution of the system until it reaches a final state (see proof in the supporting materials). Thus the system evolves to minimize the adjusted perimeter between the interface of the R and B agents. The final states are precisely the local minimizers of the Lyapunov function, subject to the threshold constraint. This Lyapunov function is also the Hamiltonian for a related spin lattice system related to the Ising model (5).

In Fig. 3, we plot average values of aggregation measures (2)-(5) introduced above for the final states with  $T = 3, 4, 5$  and several values of  $v$ . The linear relationships of these disparate aggregation measures on population density seems remarkable.

## 4.2 Global Aggregation Dependence on $T$

From Fig. 2, one observes that: (i) the final states with  $T = 3$  are very sparse, with a great deal of interweaving between both kinds of agents and vacant spots; (ii) the final states with  $T = 4$  consist of compact clusters (that look like “solid” objects); and, finally, (iii) the final states with  $T = 5$  consist of one (for each type) huge cluster together with a small number of remaining agents scattered around. Varying the density  $v$  does not radically alter the qualitative structure of the final states. We now quantify the aggregation for each value of  $T$ , as  $v$  varies between 2% and 33%.

### 4.2.1 $T = 3$ : sparse clusters

The sparsity of the final states with  $T = 3$  is due, in part, to large blocks of the initial checkerboard configuration that remain unchanged during the evolution. We call this phenomenon the *super-stability* of the checkerboard. Every agent is not just happy, but has one like neighbor to “spare”. Thus, it takes a large perturbation to make a given agent move and, therefore, only agents close to the initially perturbed sites move. Consequently, Schelling required a large density of vacant spaces  $v$  (33%) to overcome checkerboard super-stability. One can see from the left column in Fig. 2 and from Fig. 5 in the supporting materials, that as  $v$  decreases, larger and larger parts of the initial configuration remain unchanged during the evolution.

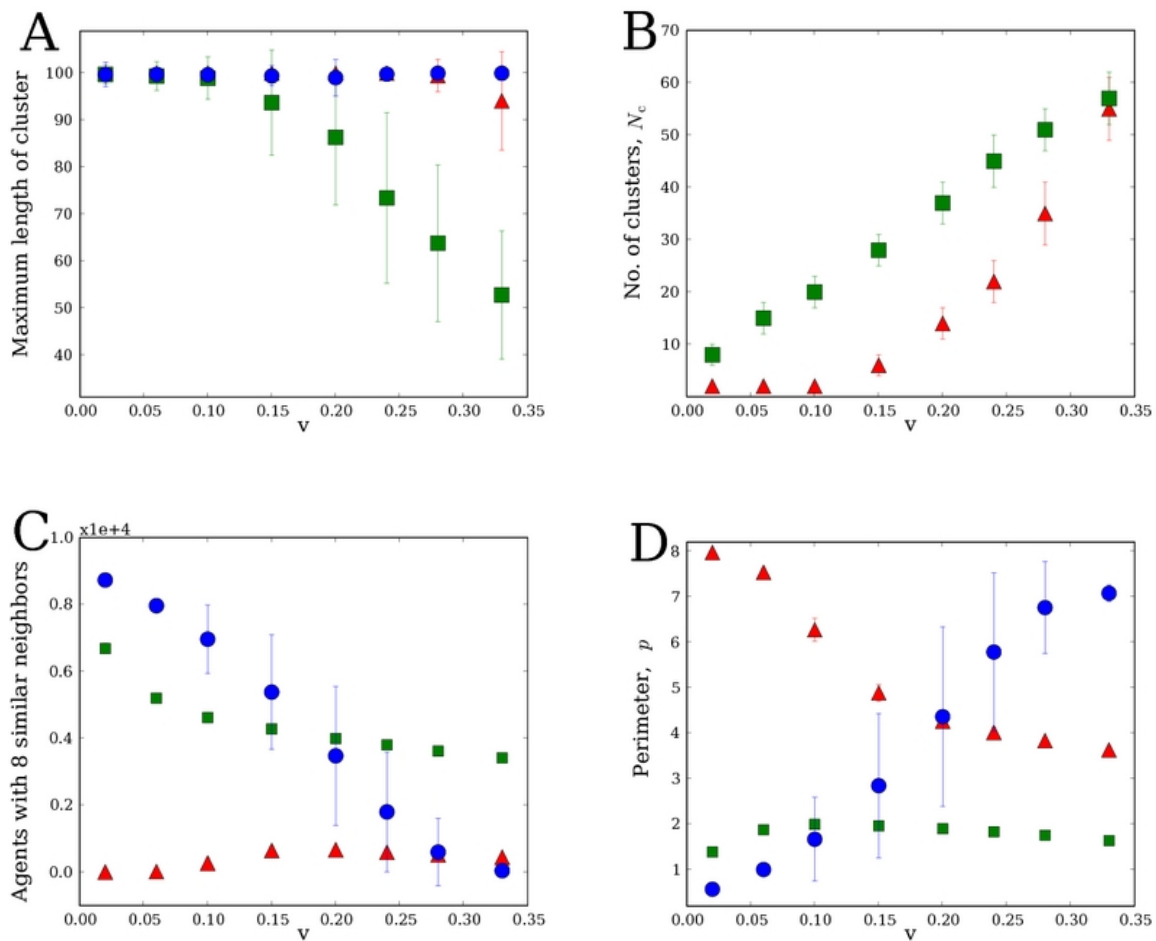


Figure 3: Statistics of four key measures of aggregation of final states for  $T = 3$  (red triangles),  $T = 4$  (green squares), and  $T = 5$  (blue circles) for different  $v$ : **A** The scale of aggregation  $L$ ; **B** The number of clusters  $N_C$ ; **C** The number of agents with eight like nearest neighbors  $N_0$ ; **D** Normalized perimeter  $p$ .

We observe that for  $T = 3$ , larger values of  $v$  result in larger clusters, and thus lead to greater global aggregation. The number of clusters in the final states,  $N_C$ , decreases as  $v$  decreases (Fig. 3B) and the dependence is almost cubic (see Fig. 9 in the supporting materials). The seclusiveness measure,  $N_0$ , is a monotonically decreasing function of  $v$ : as  $v$  decreases, the final state approaches the checkerboard and, naturally, almost all the agents have some contacts with other agents. Similarly, the smaller the value of  $v$ , the larger the normalized perimeter,  $p$ .

#### 4.2.2 $T = 4$ : compact clusters and mesoscale aggregation

Increasing  $T$  from 3 to 4 eliminates the checkerboard super-stability phenomenon and results in strikingly different structures of aggregation in final states. Namely, the final states consist of relatively small numbers, that clearly depend on  $v$ , of compact clusters (see Fig. 2D -F and Fig. 6 in the supporting materials).

For relatively large  $v$ , such final states exhibit *mesoscale aggregation* and, for small values of  $v$ , *macroscale aggregation*. There seems to be no canonical way to separate the two types of aggregation. Our criterion to define the transition when the size of the largest cluster,  $L$ , becomes equal to  $N$ .

We find two measures that clearly differentiate the global clustering of the final states for  $T = 3$  and  $T = 4$ . First, the final states have very different perimeters (see Fig. 3D). Second, for  $T = 3$ , the clusters are very sparse, while for  $T = 4$ , the clusters are compact. A natural way to quantify this is to use  $N_0$ , whose statistics we present in Fig. 3C. The measure  $N_0$  is a monotonically increasing function of  $v$ .

We quantify the differences in the final states for  $T = 4$  with  $v$  ranging from  $v = 33\%$  down to  $v = 2\%$ , with three measures: the number of clusters,  $N_C$ , the scale of aggregation,  $L$ , and the seclusiveness,  $N_0$  (Fig. 3). By providing opportunities for increasingly “easier satisfaction,” one might believe that decreasing  $v$  increases the values of  $N_C$ . Our study confirms this, and the dependence is remarkably linear. Namely, for typical final states with  $T = 4, v = 33\%$  (Fig. 2F)  $N_C$  is relatively high; for  $T = 4, v = 15\%$ ,  $N_C$  is smaller (Fig. 2E) and the clusters on average are bigger; finally, states with  $T = 4, v = 2\%$  contain only a few compact clusters of either type that stretch across the whole lattice ( $L = 100$ ). In general, as  $v$  decreases,  $L$  increases almost linearly (see Fig. 3A).

*Thus for  $T = 3$  and  $T = 4$ , the increase in  $v$  leads to the opposite effects: they increase and decrease the level of global aggregation, respectively.*

#### 4.2.3 $T = 5$ : final states with many unhappy agents

For small  $v$ , the dynamics with  $T = 5$  results in a final state achieved after just a few switches, and consists of mostly unhappy agents with no vacant space to where they could move. However, a slight modification of the selection algorithm, to allow direct R-B switches when it is not possible to switch with a vacant space, results in significant global aggregation and drastically reduces the number of unhappy agents, although not eliminating them entirely. The presence of unhappy agents in the final states is a new phenomenon, which we do not observe in simulations for  $T = 3$  (while such configurations theoretically exist, they are extremely unlikely) and



is much less pronounced for  $T = 4$  (see Fig. 8A in the supporting materials).

A typical  $T = 5$  final state with modified selection algorithm consists of one big cluster for each kind of agent and the rest of the agents are unhappy and scattered around. The smaller that the value of  $v$  is, the larger the two main clusters are and the fewer unhappy agents there are.

The globally aggregated final states (small values of  $v$ ) with  $T = 5$  (with modified selection) and  $T = 4$  (with Schelling selection) appear similar in terms of the number of large clusters and the scale of aggregation,  $L$  (Figs. 2D and G). However, there is a large difference in their perimeter  $p$ : it is much smaller for  $T = 5$  (see Fig. 3D).

## 5 Concluding Remarks

In this paper we devised new measures to quantify the aggregation in the Schelling segregation model and studied their dependence on city size, disparate neighbor comfortability threshold, and population density. We identified distinct scales of global aggregation, and showed that the striking global aggregation Schelling observed for the  $8 \times 8$  lattice is strictly a small lattice phenomenon. We also discovered several remarkable scaling laws for the aggregation measures as functions of population density.

## 6 Supporting Material

### 6.1 Schelling's Simulations

Schelling considered the cases  $N = 8$ ,  $T = 3$ , and  $v = 33\%$ . For  $T = 3$  or 4, and  $V = 0$ , a “checkerboard” configuration of B’s and R’s (imagine placing B’s on the red squares and R’s on the black squares of an actual checkerboard) is a final state, since all agents have four like nearest neighbors.

To generate his initial configurations, Schelling begins with a checkerboard configuration without periodic boundary conditions and randomly removes approximately one third of the B’s and R’s, keeping equal numbers of both agents (9). We refer to the result as a deleted checkerboard configuration. Removing these agents makes some of the remaining agents unhappy and drives the evolution. Several authors have observed that removing such a large percentage of agents is unnatural, but it is crucial to attain aggregation in Schelling’s model. Removing fewer agents results in a final configuration close to the initial configuration.

Finally, to construct his initial configurations, Schelling modifies the deleted checkerboard by randomly adding a total of 5 B’s and 5 R’s in vacant spaces. Such an initial configuration is assumed to be a proxy for a nearly integrated city.

A typical run of Schelling’s original model system (with periodic boundary conditions) is presented in Fig. 4: initial state (Fig. 4A) and final state (Fig. 4B). Schelling performed many simulations by hand using an actual checkerboard, and observed that the final states presented a significant degree of global aggregation. He equated the global aggregation with segregation of a city.

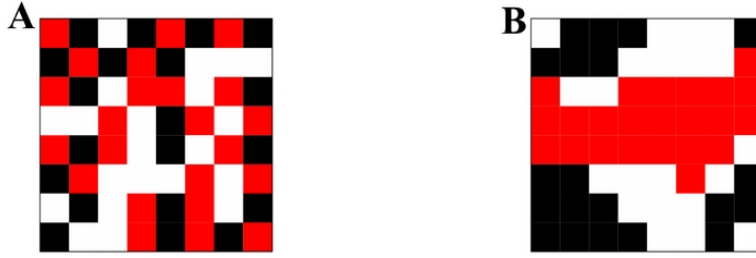


Figure 4: Schelling's original model with  $N = 8$ : **A**: initial state and **B**: final state.

## 6.2 Structure of final states for $T = 3$

In Fig. 5 we present typical final states for  $T = 3$  and different values of  $v$ . The pictures and our statistics show that as the value of  $v$  decreases, the number of clusters decreases (Fig. 3B), the final states retain larger and larger parts of the original checkerboard configuration. One can see from Fig. 5 that, unlike the final states for Schelling's original model with  $N = 8$  (see Fig. 4B) that consists of just one or two separate domains of R and B agents, the final states for  $N = 100$  and  $v = 33\%$  contain many clusters. The striking qualitative difference is also quantified by the relatively large values of the normalized perimeter,  $p$  (see Fig. 3B) and by the large differences in the values of  $N_0/N^2$  between the states presented in Fig. 3B and 4B.

## 6.3 Structure of final states for $T = 4$

In Fig. 6 we present typical final states for  $T = 4$  and different values of  $v$ . The pictures and our statistics show that as the value of  $v$  decreases, the number of clusters decreases (Fig. 3B) and the size of the compact clusters (scale of aggregation) increases (Fig. 3A).

## 6.4 Structure of final states for $T = 5$

In Fig. 7 we present typical final states for  $T = 5$  and different values of  $v$ . Observe that most of the agents away from the big clusters are unhappy (see Fig. 8 for the statistics of the unhappy agents). The pictures and our statistics show that as the value of  $v$  decreases, the number of unhappy agents in final states  $v$  decreases (Fig. 8A), and the size of a single (for each type) major cluster increases (see Fig. 8B). Another clear indication of the growth of the main cluster is the increase of  $N_0$ , presented in Fig. 3C.

The average number of unhappy agents in final states for different values of  $T$  and  $v$  is presented in Fig. 8A. It is remarkable that the average number of unhappy agents is almost a linear function of  $v$ , between  $v = 10\%$  (where they constitute approximately 10%) and  $v = 30\%$  (where they constitute approximately 33%, in other words, almost every agent). While the existence of unhappy agents in the final state does not significantly increase the perimeter  $p$  of the final states, it greatly inflates the total number of clusters  $N_C$ .

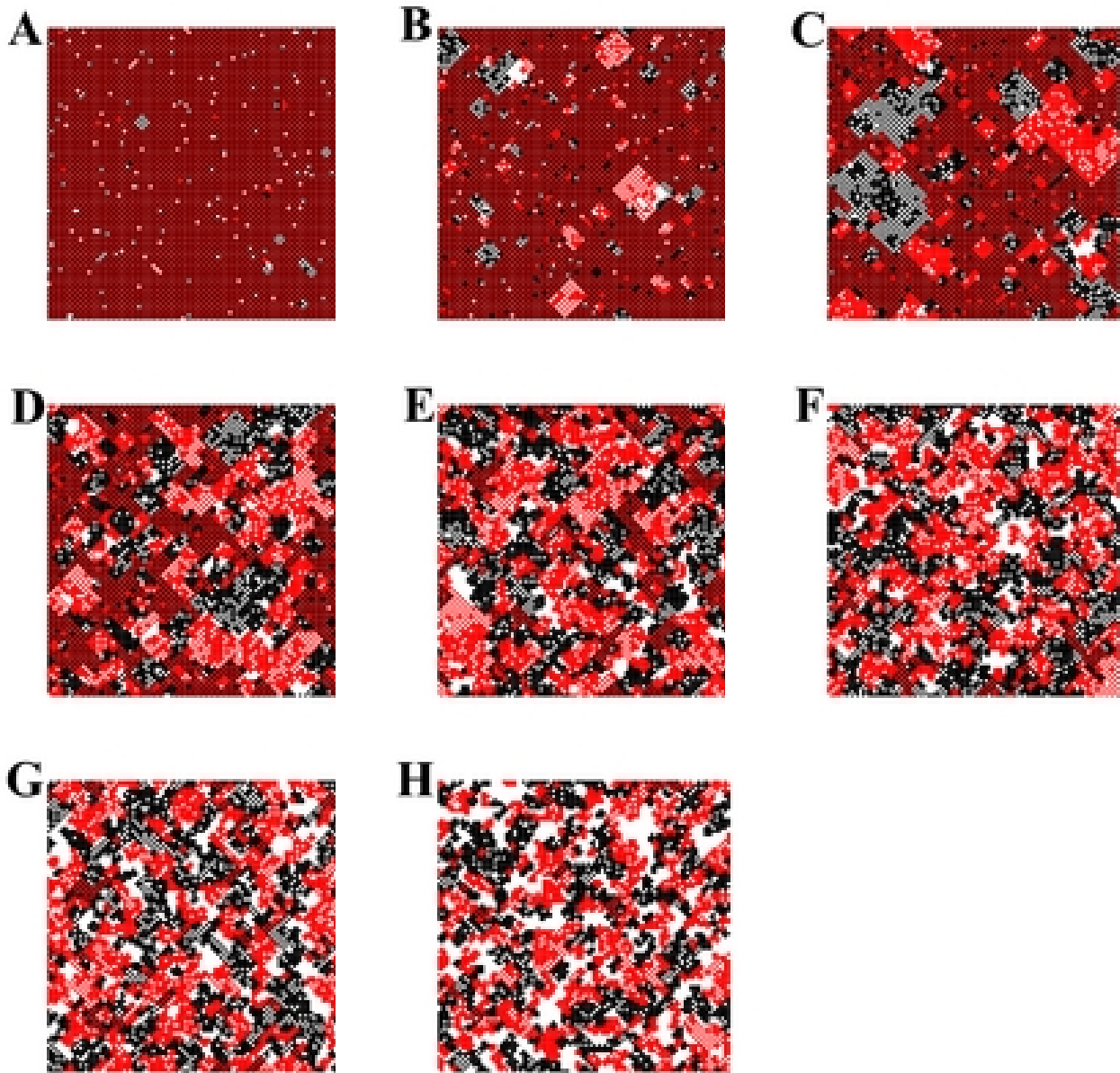


Figure 5: Characteristic final states for  $T = 3$  for different  $v$ : **A**:  $v = 2\%$ , **B**:  $v = 6\%$ , **C**:  $v = 10\%$ , **D**:  $v = 15\%$ , **E**:  $v = 20\%$ , **F**:  $v = 24\%$ , **G**:  $v = 28\%$ , **H**:  $v = 33\%$ .

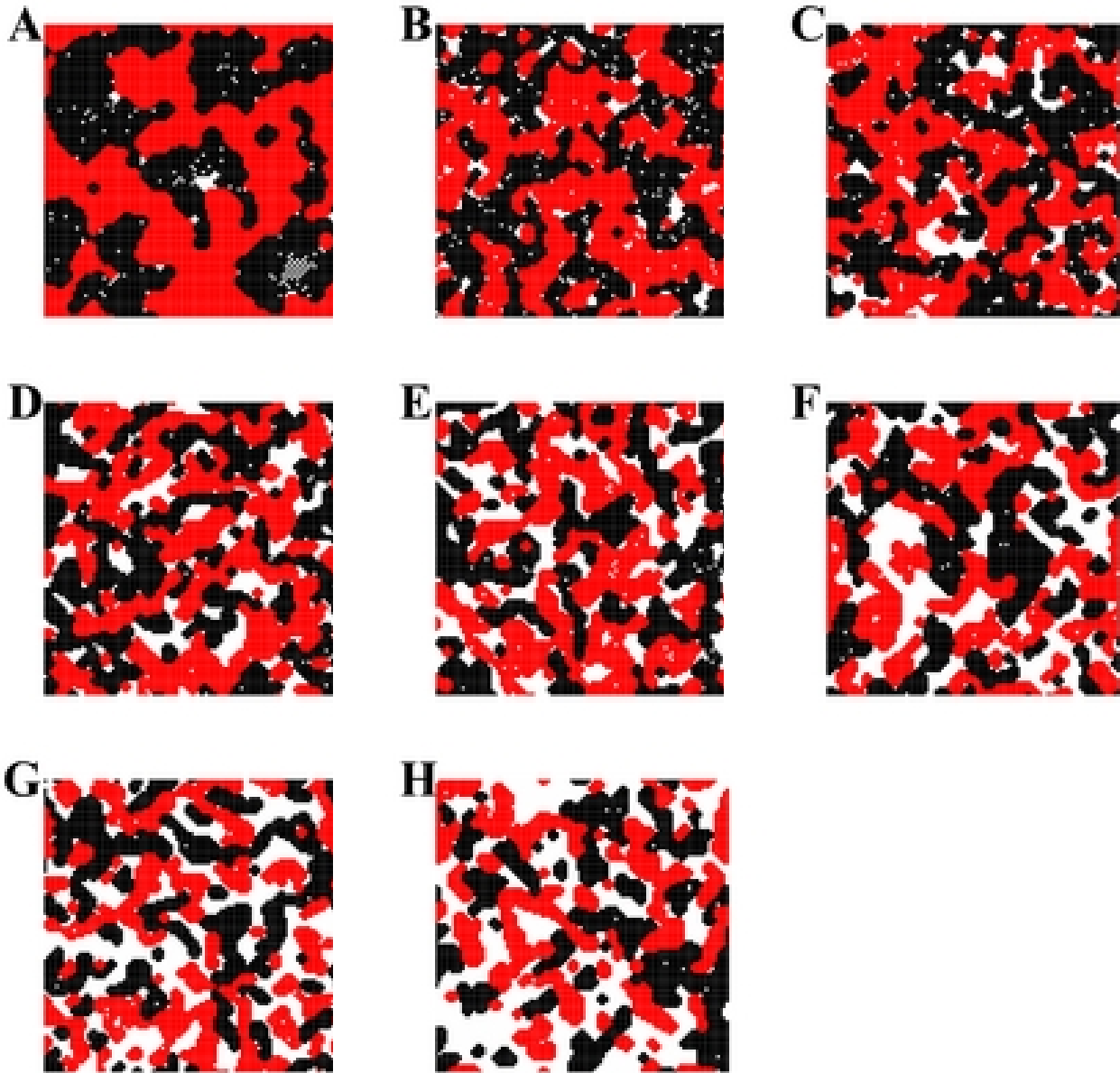


Figure 6: Characteristic final states for  $T = 4$  for different  $v$ : **A**:  $v = 2\%$ , **B**:  $v = 6\%$ , **C**:  $v = 10\%$ , **D**:  $v = 15\%$ , **E**:  $v = 20\%$ , **F**:  $v = 24\%$ , **G**:  $v = 28\%$ , **H**:  $v = 33\%$ .

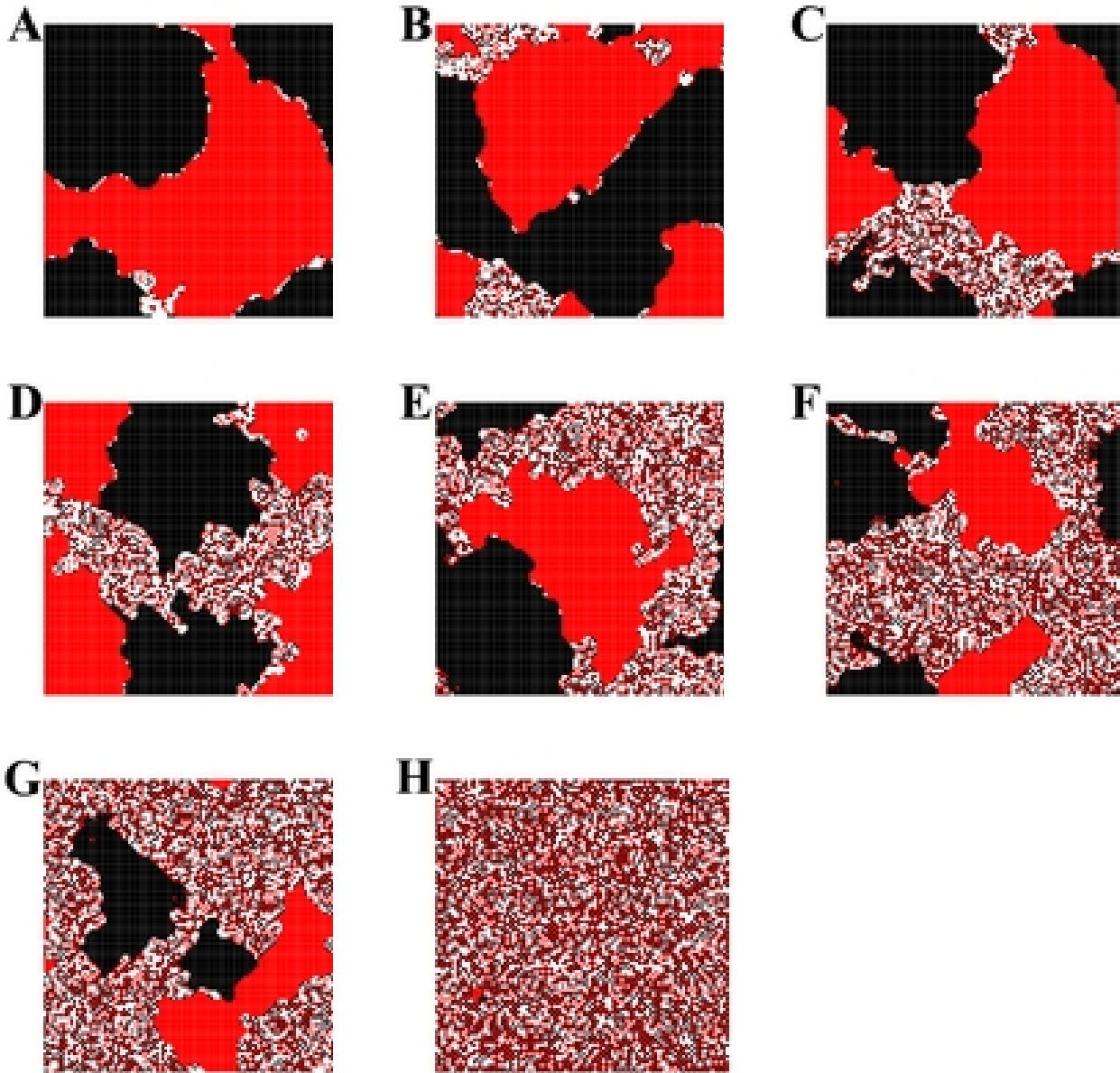


Figure 7: Characteristic final states for  $T = 5$  for different  $v$ : **A**:  $v = 2\%$ , **B**:  $v = 6\%$ , **C**:  $v = 10\%$ , **D**:  $v = 15\%$ , **E**:  $v = 20\%$ , **F**:  $v = 24\%$ , **G**:  $v = 28\%$ , **H**:  $v = 33\%$ .

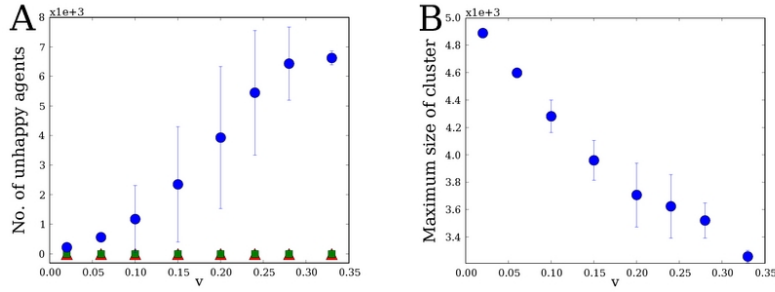


Figure 8: Statistics of the final states with  $T = 5$ : **A**: The average number of unhappy agents in final states for  $T = 3$  (red triangles),  $T = 4$  (green squares), and  $T = 5$  (blue circles); **B**: The average number of the agents in the two big clusters.

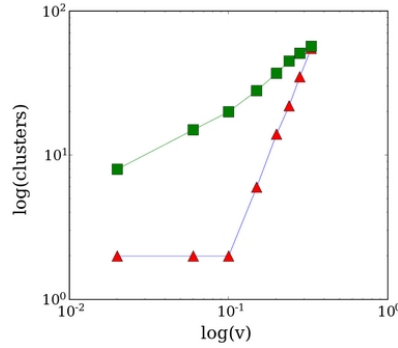


Figure 9: Statistics of the number of clusters in the final states for  $T = 3$  (red triangles),  $T = 4$  (green squares) for different  $v$  on a log – log scale.

## 6.5 Statistics of the number of clusters

In Fig. 9 we replot the data shown in Fig. 3B on a log scale (to illustrate power-law statistics), showing the statistics of the number of clusters in the final states for  $T = 3$  and  $T = 4$ , for different  $v$ . The lines indicate power laws. The values for the slopes are 0.89 for  $T = 4$  (the value 1 is well within the error bars) and 2.76 for  $T = 3$  (the value 3 is well within the error bars).

## 6.6 Number of steps in the evolution

The average number of switches required for the final state to be achieved are (3596, 5192, 5573, 4422) respectively, for  $T = 3, v = 33\%$ ;  $T = 4, v = 33\%$ ;  $T = 4, v = 2\%$ ; and  $T = 5, v = 2\%$ . The switches for  $T = 5, v = 0.02$  that included both R and B agents are counted twice. The most striking feature is that it takes significantly fewer switches to achieve the final state for  $T = 5$  than for  $T = 4$ . The distribution of the number of jumps for different agents is presented in Fig. 10.

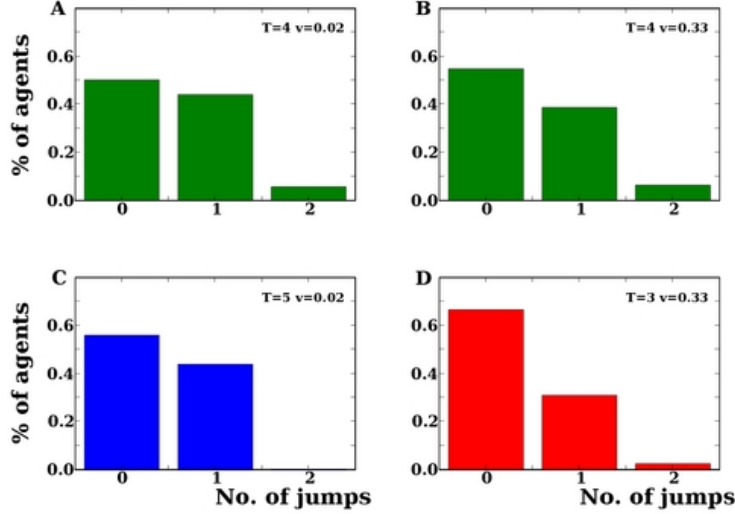


Figure 10: Statistics of the number of agent jumps.

## 6.7 Final states with $N = 50$ and $N = 200$

To illustrate the dependence of the final states of  $N$ , we performed the simulations for  $N = 50$  and for  $N = 200$ . Characteristic final states are presented in Fig. 11 and Fig. 12 for  $N = 50$  and  $N = 200$ , respectively. One can see that both figures are qualitatively very similar to Fig. 2.

## 6.8 Measures of Aggregation

Schelling considered two quantities to measure the aggregation of a state:

1. The ratio of unlike to like neighbors is called the  $[u/l]$ -measure. For a site on the final lattice with coordinates  $(i, j)$ , we define:

$$[u/l]_{i,j} = \frac{q_{i,j} + w_{i,j}}{p_{i,j}},$$

where  $p_{i,j}$ ,  $q_{i,j}$ , and  $w_{i,j}$  are the number of like, unlike, and vacant neighbors of the agent located at  $(i, j)$ , respectively. We define the *sparsity*  $\langle [u/l] \rangle$  of a cluster by averaging the  $[u/l]$ -measure over the given cluster.

2. The number of agents that have neighbors *only* of the same kind,  $N_0$  (note, that this definition excludes the vacant spaces as well). The abundance of such agents indicate the presence of large, “solid” clusters. This quantity is the most useful in quantifying between the states with  $T = 3$  and  $T = 4$ .

Besides those two characteristics, we introduce several more.

3. The total number of clusters,  $N_C$ . With 8-point neighborhoods, clusters may be intermingled. For example, a checkerboard configuration has just  $1 + 1 = 2$  clusters. The quantity  $N_C$  is

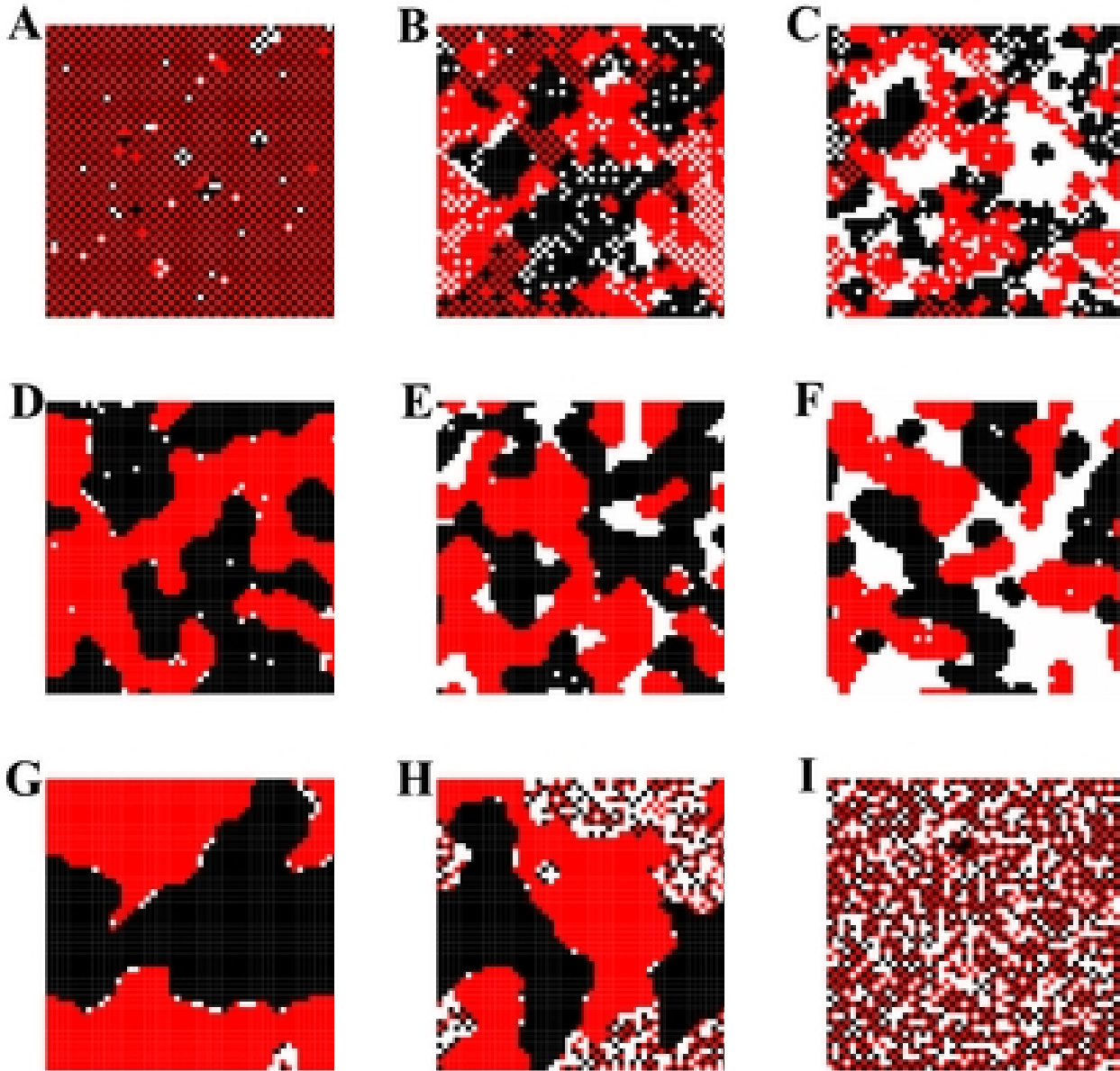


Figure 11: Characteristic final states for  $N = 50$  and different values of  $T$  and  $v$ : **A**:  $T = 3$ ,  $v = 2\%$ , **B**:  $T = 3$ ,  $v = 15\%$ , **C**:  $T = 3$ ,  $v = 33\%$ , **D**:  $T = 4$ ,  $v = 2\%$ , **E**:  $T = 4$ ,  $v = 15\%$ , **F**:  $T = 4$ ,  $v = 33\%$ , **G**:  $T = 5$ ,  $v = 2\%$ , **H**:  $T = 5$ ,  $v = 15\%$ , **I**:  $T = 5$ ,  $v = 33\%$ .



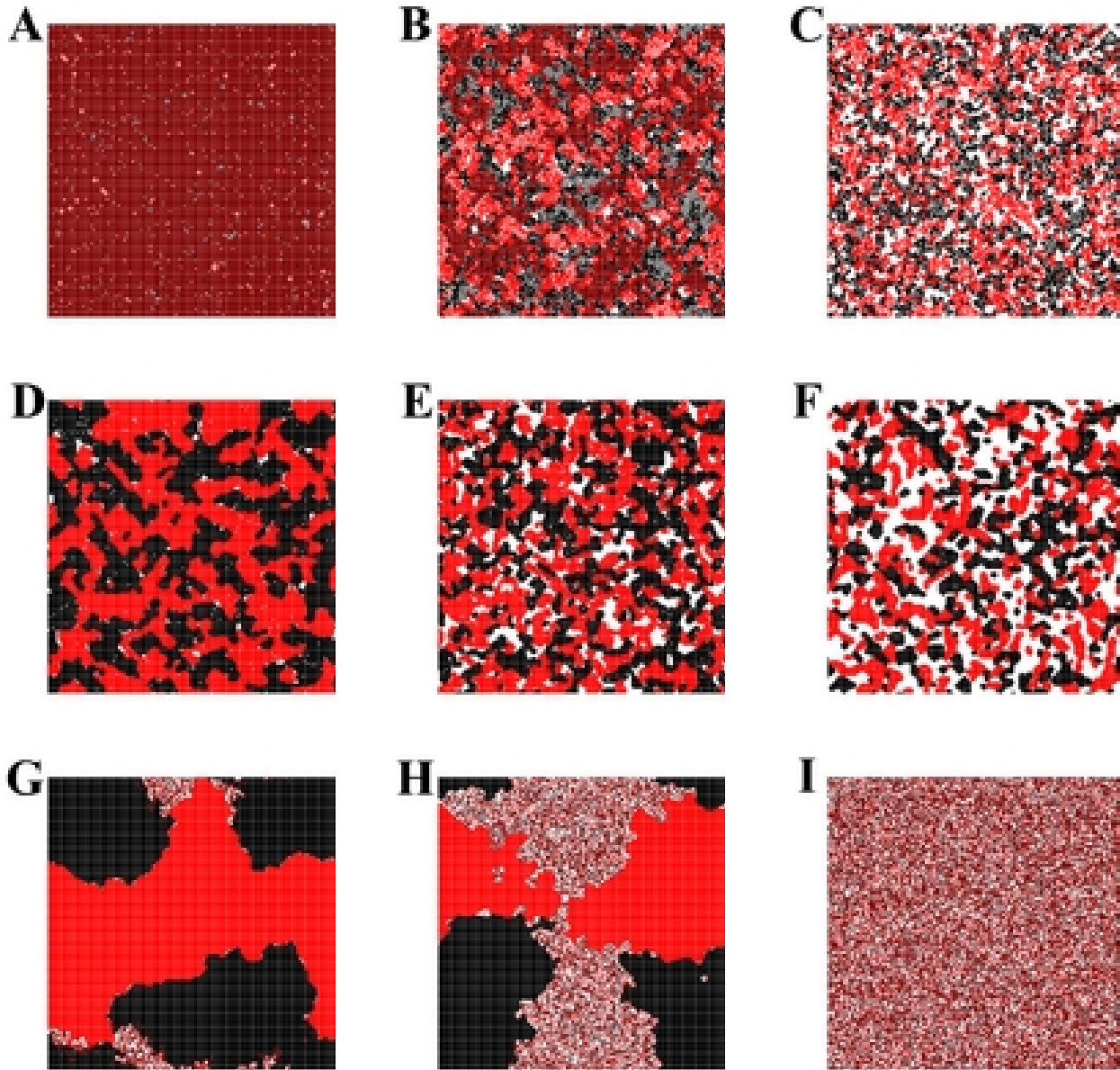


Figure 12: Characteristic final states for  $N = 200$  and different values of  $T$  and  $v$ : **A**:  $T = 3$ ,  $v = 2\%$ , **B**:  $T = 3$ ,  $v = 15\%$ , **C**:  $T = 3$ ,  $v = 33\%$ , **D**:  $T = 4$ ,  $v = 2\%$ , **E**:  $T = 4$ ,  $v = 15\%$ , **F**:  $T = 4$ ,  $v = 33\%$ , **G**:  $T = 5$ ,  $v = 2\%$ , **H**:  $T = 5$ ,  $v = 15\%$ , **I**:  $T = 5$ ,  $v = 33\%$ .

the most useful for configurations consisting of compact clusters of a similar size. To study configurations such as the final states for  $T = 5$ , a more useful quantity is the number of clusters that have greater than, say,  $M_{max}/10$  agents, where  $M_{max}$  is the number of agents in the largest cluster of a given kind.

4. Total perimeter (normalized by the number of agents). For  $v \neq 0$ , we follow the calculation of surface tension in the physics of foams, and write

$$p = \frac{P}{N^2} = \frac{1}{N^2} \sum_{i,j=1}^N (q_{i,j} + w_{i,j}/2).$$

Thus defined,  $P$  plays the role of a *Lyapunov function*: it can be shown that in the process of evolution every legal switch makes  $P$  smaller.

Suppose we switch an R and a V. Before the switch, suppose R had  $B_1$ ,  $R_1$ , and  $V_1$ , of B, R, and V neighbors, respectively. Similarly, the numbers for the V agent are  $D_2$ ,  $R_2$ , and  $V_2$ . Then the value of  $P$  before and after the switch are:

$$P_{initial} = 2B_1 + V_1 + B_2 + R_2; \quad P_{final} = 2B_2 + V_2 + B_1 + R_1.$$

Thus,

$$P_{final} - P_{initial} = B_2 + V_2 + R_1 - (B_1 + V_1 + R_2).$$

Taking into account that  $B_1 + V_1 + R_1 = B_2 + V_2 + R_2 = 8$ , we arrive at

$$P_{final} - P_{initial} = 2(R_1 - R_2) < 0.$$

Similarly, if the switch between R and B, we have

$$P_{final} - P_{initial} = 2(R_2 - R_1) + 2(B_1 - B_2) < 0.$$

5. We define the *diameter of a cluster*,  $L$ , to be the side length of the smallest square that covers the cluster. The diameter of a cluster can be easily computed as the larger between the number of rows that contain an agent belonging to the cluster and the number of columns that contain an agent belonging to the cluster. For configurations consisting of mostly compact clusters, the maximum diameter,  $L = \max(L_i)$ , defines the *scale of aggregation*.

## References and Notes

- [1] I. Benenson, E. Or, E. Hatna, I. Omer, *Residential Distribution in the City Reexamined*, in press.
- [2] E. Bruch, R. Mare, *Neighborhood Choice and Neighborhood Change*, AIS **112**, 667-706, 2006.

- [3] M. Pollicott and H. Weiss, *The Dynamics of Schelling-Type Segregation Models and a Nonlinear Graph Laplacian Variational Problem*, *Advances in Applied Mathematics* **27**, 17-40 (2001).
- [4] <http://www.realestateagent.com/glossary/real-estate-glossary-show-term-1699-occupancy-ratio.html>.
- [5] B. Simon, *The Statistical Mechanics of Lattice Gases*, Vol 1, PUP, 1993.
- [6] T. Schelling, *Models of Segregation*, *American Economic Review* **59**, 488–493, 1969.
- [7] T. Schelling, *On the Ecology of Micromotives*, *The Public Interest* **25**, 61–98, 1971.
- [8] T. Schelling, *Dynamic Models of Segregation*, *Journal of Mathematical Sociology* **1**, 143–186, 1971.
- [9] T. Schelling, *Micromotives and Macrobehavior* (W.W. Norton, New York, ed.1, 1978), pp.137-166
- [10] D. Vinkovic and A. Kirman, *A Physical Analogue of the Schelling Model*, *PNAS* **103**, 19261–19265, 2007
- [11] S. Gerhold, L. Glebsky, C. Schneider, H. Weiss, and B. Zimmermann, *Limit States for One-dimensional Schelling Segregation Models*, *Commin Nonlinear Science and Numerical Simulations*, to appear.
- [12] A. Singh, D. Vainchtein, and H. Weiss, *Schelling's Segregation Model with Minorities*, In preparation.
- [13] W. A. V. Clark, *Residential Preferences and Neighborhood Racial Segregation: A Test of the Schelling Segregation Model*, *Demography*, **28**, 1–19, 1991. doi:10.2307/2061333.
- [14] R. Sander, D. Schreiber, J. Doherty, *Empirically Testing a Computational Model: Architectures and Institutions*, edited by D. Sallach and T. Wolsko, Chicago, IL: University of Chicago; ANL/DIS/TM-60, Argonne National Laboratory, Argonne, IL, 2000.